International Journal of Bioelectromagnetism
Vol. 11, No. 4, pp.161-169, 2009
www.ijbem.org

Network Parameters for Studying Functional Connectivity in Brain MEG Data

F. Di Grazia[a], F. Sapuppo[a], D. Shannahoff-Khalsa[b], M. Bucolo[a]

[a] *Dipartimento di Ingegneria Elettrica, Elettronica e dei Sistemi, Università degli Studi di Catania, Italy*

[b] *Institute for Nonlinear Science, University of California, San Diego, La Jolla, California, USA*

Correspondence: F.Sapuppo, Dipartimento di Ingegneria Elettrica, Elettronica e dei Sistemi, Università degli Studi di Catania, V.le A, Doria 6, 95125 Catania, Italy. E-mail: fsapuppo@diees.unict.it, phone +39 095 7382603, fax+39 095 330793

Abstract. The functional connectivity of various brain regions has been studied here using the knowledge from two different scientific fields. The methods of Synchronization Likelihood (SL) and network theory are applied to magnetoencephalography (MEG) data in an effort to study the brain as a complex network. In this paper the SL method has been used to characterize the functional interactions as ''functional connectivity'', by performing measures of statistical interdependencies between brain activity signals. The underlying assumption is that such correlations, at least in part, reflect the functional interactions between different brain regions. Methods applied in this study investigate the occurrence of small-world phenomenon in MEG data by considering the application of the SL method and the characterization of the respective graphs obtained by varying the threshold T.

The data set used here is from a single subject performing a yogic breathing exercise. In the results we show how we are able to characterize and differentiate the different phases of the breathing exercise by using the index σ that defines the presence of a small world network, along with other network parameters that include the clustering coefficient, the characteristic path length, and the nodes degree.

Keywords: magnetoecephalography, functional connectivity, network theory, yoga, meditation

1. Introduction

The complexity of brain dynamics is a newly emerging field [Stam C.J. 2006], and numerous techniques for the measurement and characterization of cerebral physiological activities [Kandel E.R.et al 2000] have been developed with an effort towards the understanding of the brain through both signals and images [Le van Q.M. 2003].

The developments in the theory of complex networks have motivated new applications in the neurosciences [Motter A.E. et al 2006]. Recent studies have led to important results in understanding the relationship between the structural properties of networks and the nature of the dynamics taking place in these networks [Bassett D.S. et al 2006].

The study of models of neural networks, anatomical connectivity, and functional connectivity, based on fMRI, EEG and MEG, have been determined by using graph spectral analysis [Stam C.J. et al 2007b]. This suggests that the human brain can be modeled as a complex network, and may have different structures both at the anatomical level as well that of functional connectivity. Moreover anatomical studies suggest that neural networks, ranging from the central nervous system of C. elegans [Watts D.J. et al 1998] to cortical networks in the cat and macaque, may be organized as small-world networks [Hilgetag C.C. et al. 2000]. Lago-Fernandez et al. (2000) showed that neural network models with small-world structures facilitate a fast system response and the emergence of coherent oscillations.

The method used here is based on the modern theory of networks derived from graph theory [Amaral L.A.N. et al. 2004]. It is combined here with the concept of interactions between dynamical systems that have been commonly quantified using linear techniques, eg. coherency [Nunez P.L. et al 1997], and other methods [Franaszczuk, P.J. et al 1999] like "synchronization likelihood" (SL) [Stam C.J. 2002].

In this paper the "synchronization likelihood" method has been used to characterize the functional interactions as ''functional connectivity'' [Lee L. et al 2003], by performing measures of statistical interdependencies between brain activity signals. The underlying assumption is that such correlations, at least in part, reflect the functional interactions between different brain regions. The synchronization of different regions of the brain and how these dynamics are affected by different stimuli or conscious activities has been shown to be one way of studying and comparing different brain states.

Here we employ the SL method for studying MEG data, recorded during a yogic breathing protocol as reported in section 4. The MEG acquisition system is described in section 2, along with the use of GRID architecture used to analyze the large datasets and to compute the onerous SL method. A description of the SL method and the modern network theory is reported in section 3.

The matrices of pair wise SL values, that represent the connectivity between couplets of MEG channels, have been converted to un-weighted graphs and opportunely represented by networks. These networks have been characterized, as shown in the results section, by an index σ, that takes into account the network parameters as the cluster coefficient, path length and degree. These networks parameters reflect an optimal situation associated with rapid synchronization and information transfer, minimal wiring costs, the balance between local processing and global integration that are all important when considering the neural synchronization of different brain regions [Stam C.J. et al 2007b].

The aim of our work here is to investigate the possibility of characterizing small-world architectures in networks obtained through functional connectivity studies based on spatio-temporal MEG data and to find suitable discrimination indices by combining network theory and dynamical system interaction studies of brain activity.

2. MEG Data

Advanced technological solutions have been used here for the acquisition of MEG signals and for the processing of the related spatio-temporal information that involves very large quantities of data.

3.1 MEG Acquisition System

Recordings were made using a whole-head 148-channel MEG instrument (4-D Neuroimaging, San Diego, California) located at The Scripps Research Institute (La Jolla, CA). Each of the 148 pick-up coils in this instrument is a 2-cm diameter magnetometer, with a distance of 2.2 cm between coils, center to center. Each coil is connected to a SQUID that produces a voltage proportional to the magnetic field radial to the head, resulting in preferential sensitivity to neural electrical sources tangential to the surface of the scalp emanating from cortical sulci.

This MEG system is contained in a magnetically shielded room that helps reduce the contribution of magnetic fields from more distant sources, and this significantly increases the signal-to-noise ratio and improves the ability to detect deeper signal sources in the brain. Trained MEG technicians positioned the subject, applied electro-oculogram leads, and performed head shape digitization. An individual was employed who is highly trained with yogic breathing techniques and in being a subject for MEG studies. Head-shape was digitized, based on known locations on the subject's head (tragus of left and right ears and nasion). Head shape data is for later co-registration between measurement coil locations, electrode locations, and scalp landmarks. Eye movements were recorded with electrodes placed above and below the right eye. Electrode impedances were set below 5 kohms. MEG data was recorded with a sampling rate of 254 Hz, with an analog filter band pass of 1 to 100 Hz.

3.2 Parallel processing: GRID Architecture

The data processing of MEG spatio-temporal datasets has been carried out on GRID parallel architecture. The computational burden of one data set channel consists of 15240 samples/minute with a sampling rate of 254Hz) and the use of computational onerous methods as the theory of networks combined with the synchronization likelihood(SL) method, that will be described in the methodology section, has led to the necessity of using grid technologies. Distributed computing turns out to be a very powerful approach to help speed up simulations and process these very large quantities of data compared to a more conventional approach in which the reduction of the spatial and temporal dimension was necessary.

In this application a Matlab code was translated to machine code in order to be executed successfully over the Unix GRID environment. Due to the complexity of the computations, a divide and conquer approach has been employed: the source dataset is recursively divided to simplify the original problem, without losing any generality and/or precision. The datasets have been split into small chunks to balance the load of every node involved in the simulation. Remote storage elements have been used to support the very large quantities of data for further processing.

3. Methods

In this paper the "synchronization likelihood" method has been used and combined with the network theory to characterize the functional interactions as ''functional connectivity''. Methods applied in this study investigate the occurrence of small-world phenomenon in MEG data by applying the SL method and the characterization of the respective graphs obtained by applying a threshold T to the SL matrix in order to obtain adjacent matrices represented by networks.

4.1 Synchronization Likelihood methods

Synchronization Likelihood is a general measure of the degree of linear and non-linear coupling between two channels [Stam CJ, Van Dijk BW2002]. Let us consider M simultaneously recorded time series x_k with length of N, where k denotes channel number (k = 1, . . ., M). The first step in the computation of the SL is to convert the series related to each channel k in a matrix X_k in which the rows are the time series of state space vectors obtained using the method of time delay embedding [Takens F. 1981], where L is the time lag, m the embedding dimension and $x_{k,i}$ represents the starting point of the series where i = 1,2,..., N-(m-1)*L as reported in equation (1).

$$X_{k,i} = (x_{k,i}, x_{k,i+L}, x_{k,i+2L}, \ldots, x_{k,i+(m-1)xL}) \tag{1}$$

Assuming two generic different channels and their related matrices X and Y, SL is defined as the conditional likelihood that the distance between Y_i and Y_j is smaller than a cut-off distance r_y, given that the distance between X_i and X_j is smaller than a cut-off distance r_x. In the case of maximal synchronization, this likelihood is equal to 1; in the case of independent systems, it is a small number P_{ref}, different from zero. This number is the likelihood that two vectors, randomly chosen, Y_i (or X_i) are closer than the cut-off distance r. To understand how P_{ref} is used to fix r_x and r_y, it is necessary to consider, at first, the correlation integral of a specific channel k, identified by X:

$$C_r = \frac{2}{N(N-\omega)} \sum_{i=1}^{N} \sum_{i+w}^{N-\omega} \theta(r - |X_i - X_j|). \tag{2}$$

Here the correlation integral Cr is the likelihood that two randomly chosen vectors are closer than r. The |.| operator represents the Euclidean distance between the vectors, N is the number of vectors, w is the Theiler correction for autocorrelation [Theiler J. 1986], and θ is the Heaviside function: θ(X)=0 if X>0 and θ(X)=1 if X<0. At this point r_x is chosen such that $C_{rx} = P_{ref}$, and r_y is chosen such that $C_{ry} = P_{ref}$. The SL between X and Y can now be formally defined as:

$$SL = \frac{2}{N(N-\omega)P_{ref}} \sum_{i=1}^{N} \sum_{j=i+w}^{N-\omega} [\theta(r_x - |X_i - X_j|)\theta(r_y - |Y_i - Y_j|)]. \tag{3}$$

SL is a symmetric measure of the strength of synchronization between X_i and Y_i. In the equation (3), the average is calculated over all i and j. From equation (3), it can be seen that in the case of complete synchronization SL=1; in the case of complete independence SL=P_{ref}. In the case of intermediate levels of synchronization P_{ref}<SL<1.

The SL method gives a synchronization matrix that is a square matrix where the x axis and the y axis correspond with the channel numbers, and where the entries indicate the strength of the SL between specific pairs of channels.

4.2 Network Theory

The SL matrix can be built using pair wise SL values for each couplet of head channels, then it is converted to an un-weighted graph where the nodes represent the channels and where, by applying a specific threshold, an edge was created between those nodes having a SL value above the threshold, and no edge in the case of a sub-threshold SL.

The resulting graphs can be easily characterized through parameters such as the clustering coefficient *Cp*(i), the characteristic path length *Lp*(i) and the degree k(i) calculated for the node ith and then extended to the entire network as *Cp*, *Lp* and k, averaging them over all nodes. In particular, the clustering coefficient is defined as the measure of the local interconnection of the graph, where the path length is an indicator of its overall connection that suffers for disconnected nodes in the graph [De Vico Fallani et al., 2007], thus only the subconnected graphs were considered for its calculation in the present work. Watts and Strogatz (1998) have shown that graphs with many local connections and a few random long distance connections are characterized by a high cluster coefficient and a short path length; the networks having these properties are known as ‘‘small-world.’’ With a probability p, a random edge is chosen and rewired to be connected to a randomly chosen vertex. By varying p between 0 and 1, different graphs can be created which span the whole range from regular (p = 0) to random (p= 1).

Regular networks of N nodes have a high *Cp* (*Cp* ≈ 3/4) but a long characteristic path length (*Lp* ≈ N/2*k*); random graphs have a low *Cp* (*Cp* ≈ *k*/N) but the shortest possible path length (*Lp* < ln(N)/ln(*k*)). Thus, the discovery of Watts and Strogatz proves that networks with 0 < p < 1 have a path length that is much smaller than that of a regular network, while the *Cp* is still close to that of a regular network. Assuming that $\gamma = C_{network}/C_{rand}$, $\lambda = L_{network}/L_{rand}$, $\sigma = \gamma / \lambda$ the small-world networks are characterized by having $\gamma > 1$ and $\lambda \approx 1$, thus $\sigma \geq 1$. These parameters are thus a good indicator of the presence of a small-world phenomenon. Many types of real networks have been shown to have small-world features [Strogatz S.H. 2001]. Moreover, different patterns of anatomical connectivity in neuronal networks show a high clustering and a small path length [Watts D.J. et al 1998].

4. Case Study: Yogic protocol

The subject was recorded while reclining and supported at 45 degrees. He followed a well-practiced protocol that involves a 10 minute resting baseline recording period (rest phase I), followed by a 31 minute exercise recording period, followed by a second 10 minute resting recording period (rest phase II), see Figure 1. The three phases are separated by a one-minute recording pause. The exercise phase consists of selectively breathing through only one nostril (using a plug for the other nostril, with both arms resting in the lap) at a respiratory rate of one breath per minute for 31 min that uses a repeating pattern of 15s slow inspiration, 15s breath retention, 15s slow expiration, and 15s breath hold out) [F. Sapuppo et al 2006, Shannahoff-Khalsa, D. 2007]. The left nostril version of this specific yogic technique has proven to be effective in the treatment of obsessive compulsive disorder [Shannahoff-Khalsa D. et al 1999].

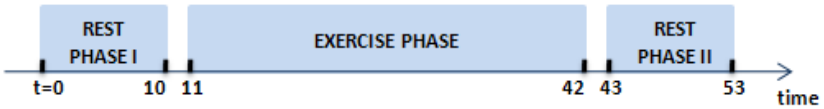

Figure 1. *Yogic Protocol Timeline.*

On day one the technique employing the left nostril is used, and on the following day, the same pattern was employed using only the right nostril. This approach is used to study the potential differential brain effects that may result from these two unique meditation techniques, and to help insure that the effects of one technique do not carry over into the effects of the other that may occur if both techniques were practiced on the same day. Three two-day experiments are repeated with a time lag of approximately one month. The dates of the left and right nostril recordings are presented in Table 1.

Table 1. *Experimental data sets over a three-month time period*

Left nostril	Right nostril
June 13, 2000 – (dataset 5)	June 14, 2000 – (dataset 6)
July 18, 2000 – (dataset 7)	July 19, 2000 – (dataset 8)
August 8, 2000 – (dataset 9)	August 9, 2000 – (dataset 10)

5. Results

The first step is the characterization of the parameters needed for the SL methods to be applied to all the six datasets. The P_{ref} value has been set equal to 0.01, and the Theiler correction w has been considered null, to be comparable with the SL method as applied in other studies [Stam C.J. et al 2007a]. The embedding parameters have been evaluated using TISEAN [Hegger R. et al 1999]. The distributions density of the time lag L and of the embedding dimension m, evaluated for each signal, have been executed in order to choose the same values for each time-series. According to the L and m distributions, the time lag has been set equal to L=5 and the embedding dimension equal to m= 6 for all time series.

SL matrices were built for each dataset exploiting GRID processing potentialities. The conversion of such SL matrices to graphs were performed varying the threshold T in the range [min(SL); max(SL)] and network parameters as Cp and Lp where used as functions of degree k. In particular the σ parameter was investigated as brain activity discriminator using threshold T varying in the range [0.8; 1]. This range has been chosen since it contains the most frequently occurring values, as can be seen in the histogram representing the SL matrix value distributions for the minute 1 of dataset 5 (figure 2).

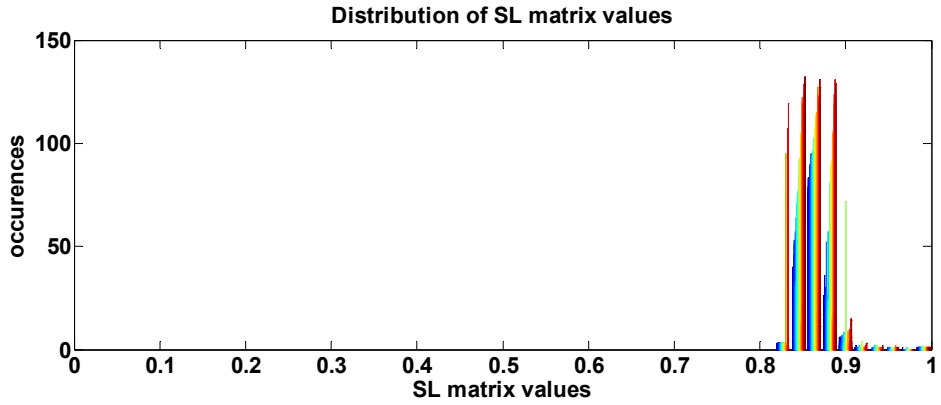

Figure 2. *Distribution of SL matrix values of minute 1 of dataset 5.*

Figure 3 shows the percentage of small-world networks (y-axes) in the three phases of the protocol over the T variation (x-axes), and it is possible to distinguish dynamics not easily detectable that are characteristic of a specific functional brain characterization and also the different behavior of the phases in the six datasets.

For the range [0.9; 1] in the exercise phase, the percentage of small-world networks is always less than in the other two phases. Moreover, for all cases the percentage of small-world networks in the exercise phase is always less than that in the rest phase 2. Meanwhile for T varying in the range [0.8; 0.9] it is possible to see that for the datasets 5, 7, and 9 with breathing through the left nostril the percentage of small-world networks in the exercise phase is always bigger than in the other two phases, while for datasets 6, 8, and 10 it is not so well defined.

Furthermore for T around 0.84 there is a discontinuity in the percentage of small world networks that rapidly rises from 0 to 100 of the percentage value. Thus, the range [0.83; 0.86] has been studied here looking at the behaviour of the σ parameter over the 51 minutes. In figure 4 the σ dynamics for the dataset 6 is reported, as an example, for the thresholds T=[0,815; 0,835; 0,845] and it possible to notice that for T=0.845 the time variation of the parameter σ has a bigger dynamic than in the other cases. Therefore, this value of the threshold has been chosen to compare the 6 datasets. For values of T slightly over 0.845 the dynamics is unchanged compared to the one obtained for T=0.845, which is predictable from the plateau in the percentage curve (figure 3).

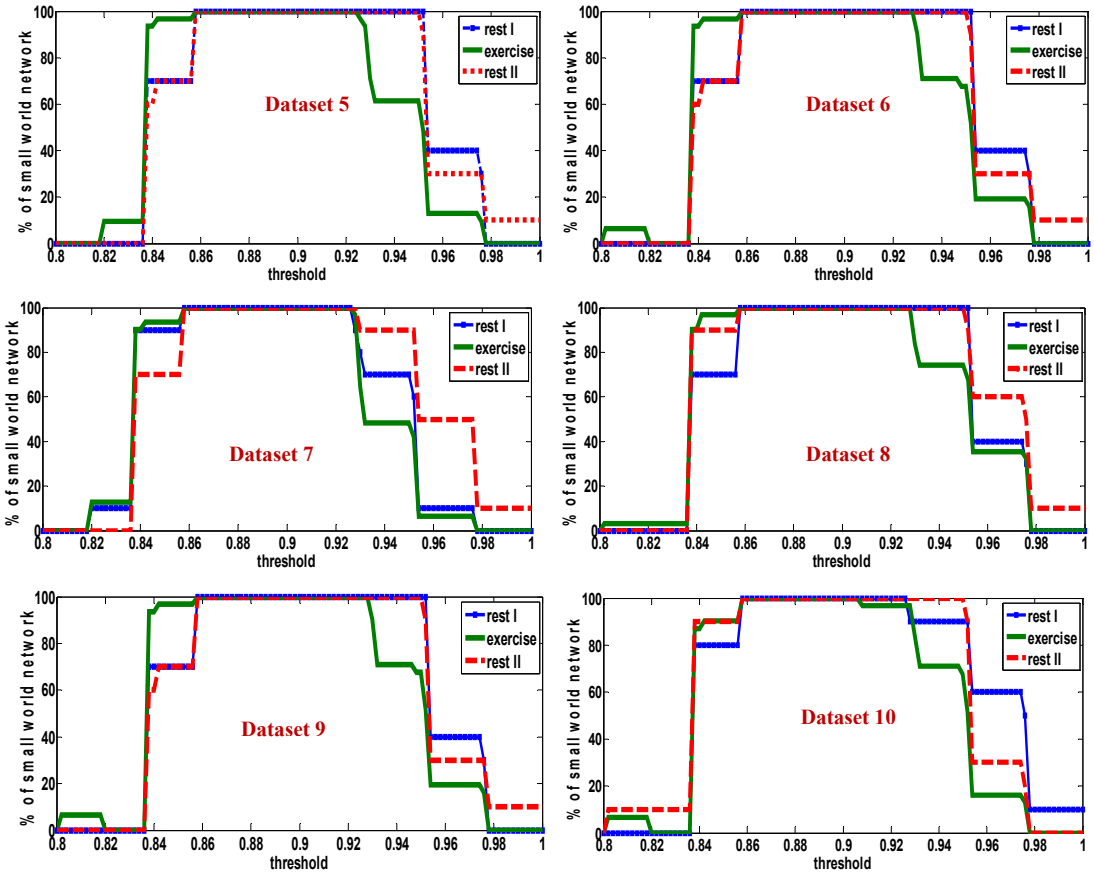

Figure 3. *percentage of small-world networks (y-axes) in the three phases of the protocol over the T variation (x-axes for both left nostril breathing (left column) and right nostril breathing (right column).*

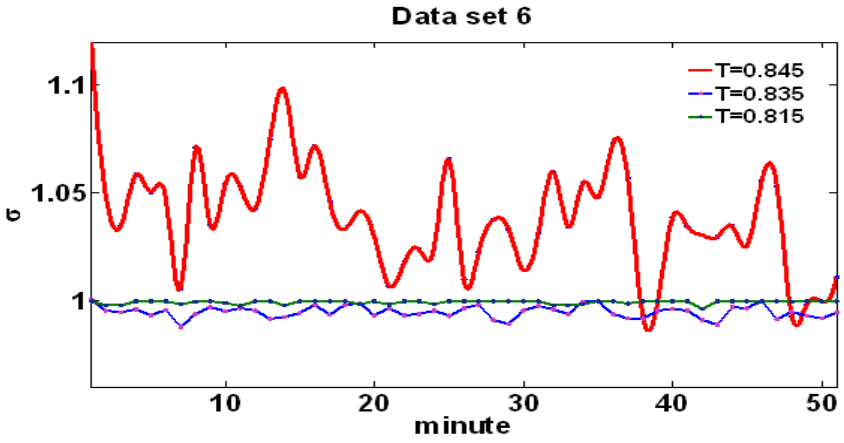

Figure 4. *σ temporal dynamics for thresholds T=[0,815; 0,835; 0,845]*

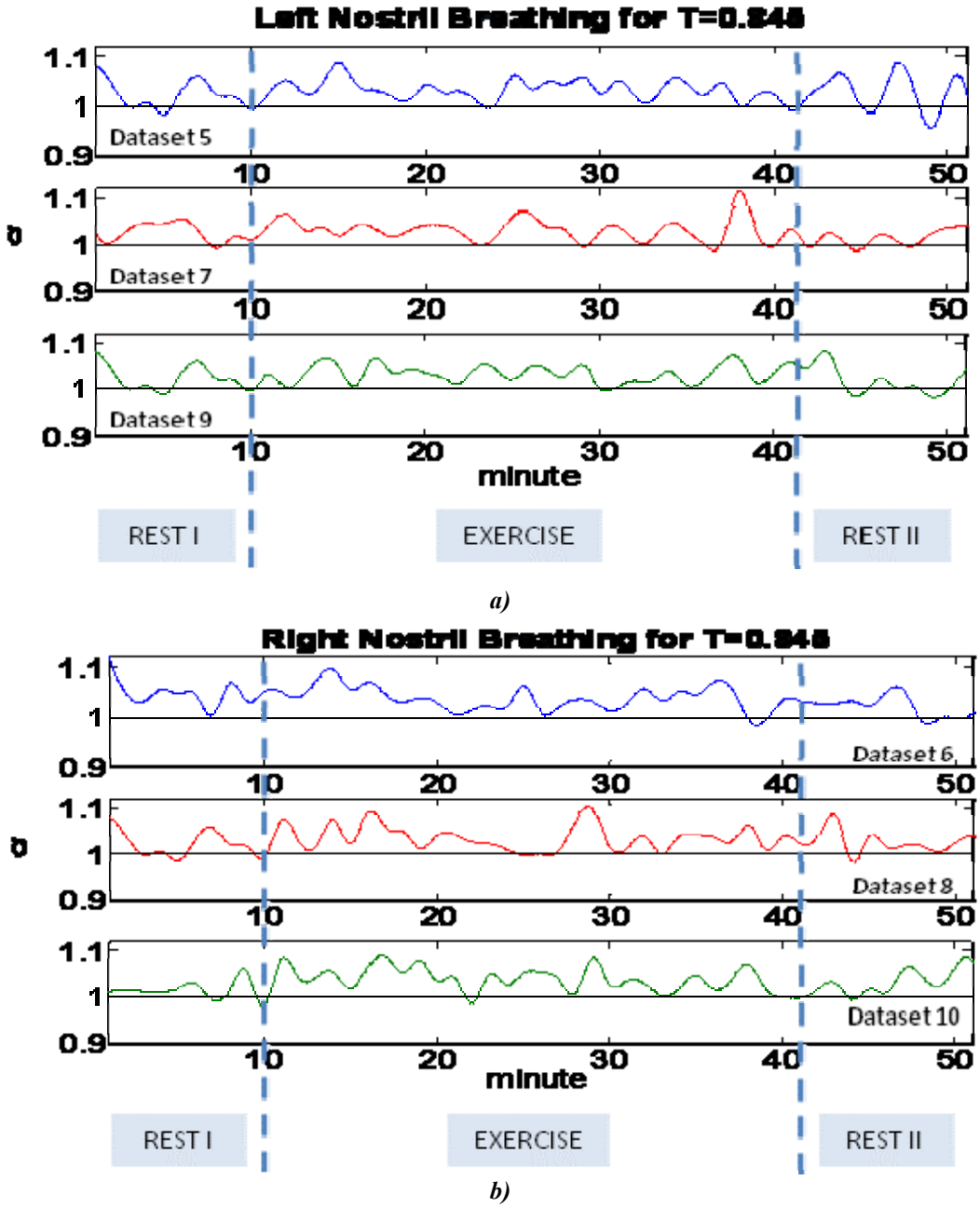

Figure 5. *σ behavior for T=0.845: a) left nostril breathing (datasets 5, 7 ,9), b) right nostril breathing (datasets 6, 8, 10).*

In addition, figure 5 shows a comparison of σ dynamics over the entire yogic protocol for all datasets. In particular figure 5a shows the cases of left nostril breathing (dataset 5, 7 ,9) and figure 5b the cases of right nostril breathing (dataset 6, 8, 10). The changes in dynamical behavior suggest the possibility of different brain organized activities that are related to the breathing activities. By visual inspection some differences in the σ dynamics can be noticed: the two rest phases (minutes [1-10] and [42-51]) seems to have slower behavior with respect to the one related to the exercise phase (minute [11-41]). This may be the result of the forced and controlled breathing activities. Histograms of the σ values related to all datasets are presented (Figure 6) and significant differences in the distributions can be noticed according to the yogic protocol phase. The trend of the σ mean values curves related to the different phases (Figure 7) shows that this parameter can discriminate different phases of the yogic protocol. Additional studies related to frequency content and to recognition of the different temporal features have to be conducted to extract quantitative consistent differences with σ dynamics in order to help better distinguish the different brain dynamics related to the two different exercises.

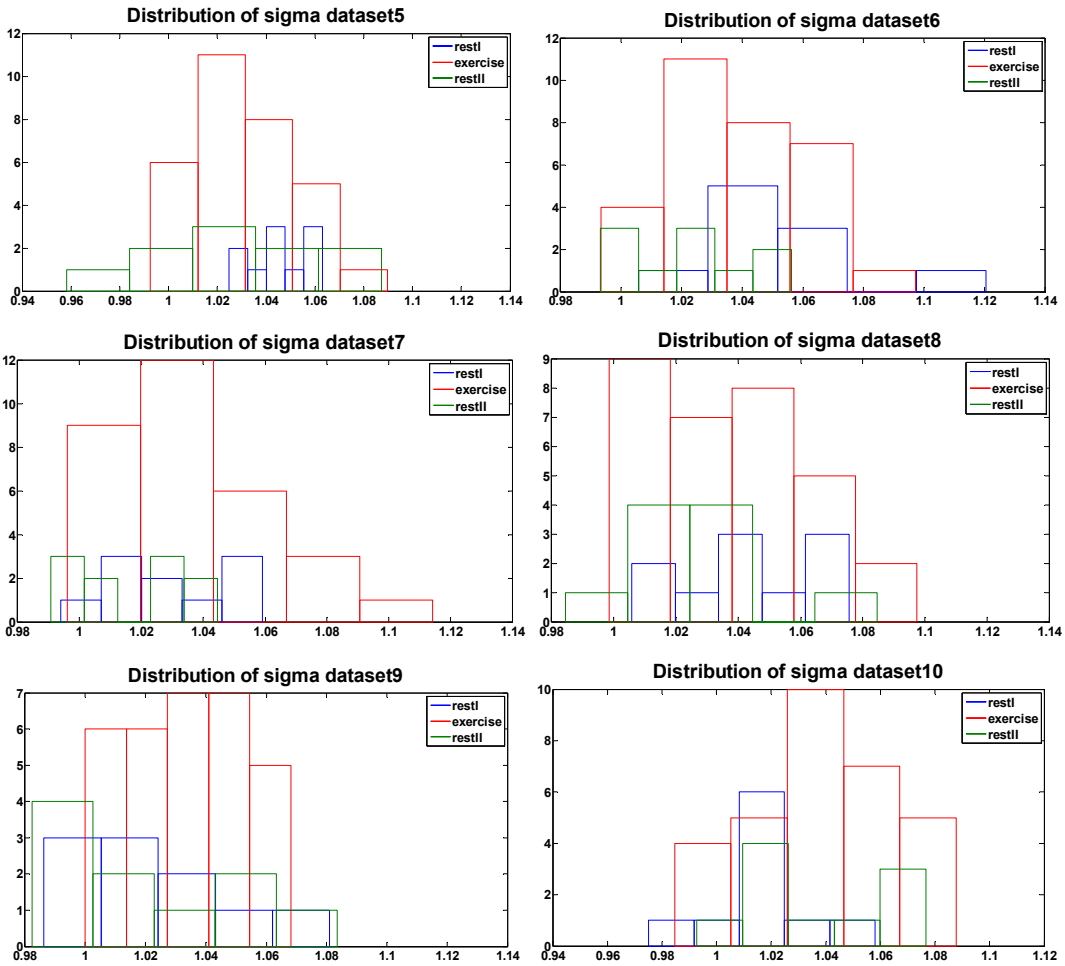

Figure 6. *Histograms of the σ values related to all datasets*

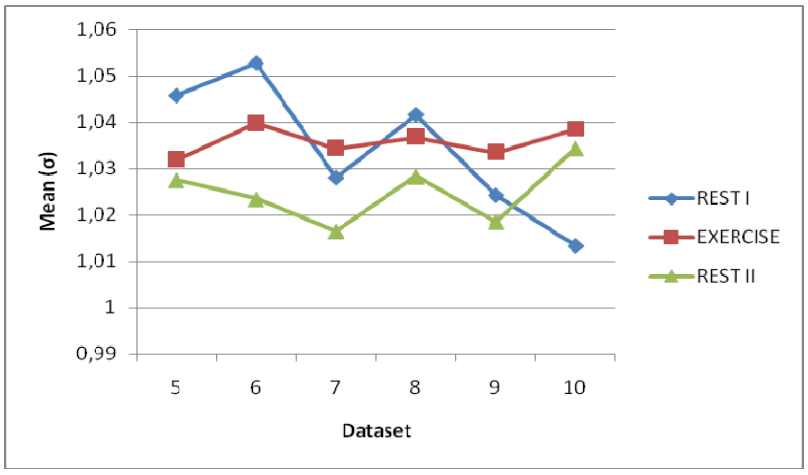

Figure 7. *σ mean values curves related to the different phases*

6. Conclusions

The effort here was directed towards the understanding of the neurophysiologic brain processes exhibited by MEG signals. The aim of this work was to investigate the possibility of finding an indicator that can help characterize and differentiate of the three phases of the yogic protocols by

examining the emerging architectures from the data analyses. The SL method has been used here to examine the statistical interdependencies amongst these signals and it has been combined with network theory. The matrices of pair-wise SL values were converted to un-weighted graphs and they have been studied and characterized by an index σ including three primary parameters: the clustering coefficient, the shortest path length, and the degree of distribution. Here we have demonstrated the possibility of extracting network architectures that can represent the functional connectivity in MEG data, or in other spatially extended bio-potentials. The use of the indicator σ, and the network parameters (Cp, Lp and k), have proven useful for characterizing the differences in the three different phases of the yogic protocol. These preliminary results suggest there is value in conducting further studies using these networks parameters. Moreover, since this specific breathing protocol includes segmented repetitions at 15s intervals, further insight to the temporal characterization of brain activity here can be represented by calculating the SL matrix and the related networks on a second timescale. Improving the time resolution of the behavior parameter calculations here may also reveal more about brain dynamics.

References

Amaral LAN, Ottino JM: "Complex networks. Augmenting the framework for the study of complex systems". *Eur Phys J B* 2004, 38:147-162.

Cornelis J Stam , Jaap C Reijneveld, Graph theoretical analysis of complex networks in the brain. *Nonlinear Biomed Phys.* 2007b ;1 (1):3 17908336

De Vico Fallani F., Astolfi L., Cincotti F., Mattia D., Marciani M.G., Salinari S., Kurths J., Gao S., Cichocki A., Colosimo A.

and Babiloni F. Cortical Functional Connectivity Networks In Normal And Spinal Cord Injured Patients: Evaluation by Graph Analysis. *Human Brain Mapping*, 28:1334-46, 2007.

Franaszczuk, P. J. and Bergey, G. K. An autoregressive method for the measurement of synchronization of interictal and ictal EEG signals. *Biol Cybern* 1999; 81:39.

Hilgetag CC, Burns GAPC, O'Neill MAO, Scannell JW, Young MP: Anatomical connectivity defines the organization of clusters of cortical areas in the macaque monkey and the cat. *Phil Trans R Soc Lond B* 2000, 355(1393):91-110.

Kandel ER, Schwartz JH, Jessell ThM: Principles of neural science McGraw-Hill; 2000.

L.F. Lago-Fernandez, R. Huerta, F. Corbacho, J.A. Siguenza, "Fast response and temporal coherent oscillations in small-world networks",*Phys. Rev. Lett.* 84 (2000) 2758–2761.

Le van Quyen M: "Disentangling the dynamic core: a research program for a neurodynamics at the large scale". *Biol Res* 2003, 36:67-88.

Lee L, Harrison LM, Mechelli A. 2003. "A report of the functional connectivity workshop, Dusseldorf 2002". *Neuroimage* 19:457--465.

P.L. Nunez, R. Srinivasan, A.F. Westdorp, R.S. Wijesinghe, D.M. Tucker, R.B. Silberstein, P.J. Cadusch, EEG coherency. I. Statistics, reference electrode, volume conduction, Laplacians, cortical imaging, and interpretation at multiple scales, *Electroenceph. Clin. Neurophysiol*. 103 (1997) 499.

R. Hegger, H. Kantz, and T. Schreiber, Practical implementation of nonlinear time series methods: The TISEAN package, *CHAOS* 9, 413 (1999).

Sapuppo F., E. Umana, M. Frasca, M. La Rosa, D. Shannahoff-Khalsa, L. Fortuna and M. Bucolo, 'Complex Spatio-Temporal Feature in MEG Data', *Mathematical Biosciences and Engineering*, October 2006, Vol. 3, No. 4, pp. 697-716.

Shannahoff-Khalsa DS, Ray LE, Levine S, Gallen CC, Schwartz BJ, Sidorowich JJ. Randomized Controlled Trial of Yogic Meditation Techniques for Patients with Obsessive Compulsive Disorders, *CNS Spectrums: The International Journal of Neuropsychiatric Medicine*, vol 4, no. 12, pp 34-46, 1999.

Shannahoff-Khalsa, DS, Selective Unilateral Autonomic Activation: Implications for Psychiatry (a review article), *CNS Spectrums: The International Journal of Neuropsychiatric Medicine*, 12(8), pp. 625-634, Aug 2007.

Stam CJ, Jones BF, Nolte G, Breakspear M, Scheltens Ph: "Small-world networks and functional connectivity in Alzheimer's disease". *Cereb Cortex* 2007, 17:92-99.

Stam CJ, Van Dijk BW. 2002. "Synchronization likelihood: an unbiased measure of generalized synchronization in multivariate data sets". *Physica D* 163:236--241.

Stam CJ: Nonlinear brain dynamics New York: *Nova Science Publishers*;2006.

Strogatz SH. 2001. Exploring complex networks. *Nature* 410:268--276.

Takens F. 1981. "Detecting strange attractors in turbulence". In: Morel JM, Takens F, Teissler B, editors. *Lecture Notes in Mathematics*. Volume 898. New York: Springer-Verlag. p 366--381.

Watts DJ, Strogatz SH. 1998. Collective dynamics of 'small-world' networks. *Nature* 393:440--442.